Electronic Supplementary Material (ESI) for Energy & Environmental Science.

Electronic supplementary information

Design guidelines for concentrated photo-electrochemical water splitting devices based on energy and greenhouse gas yields ratios

Mikaël Dumortier, Sophia Haussener

I. SHINE concentrator's CEDA and CGEA

The CEDA of the self-tracking concentrator proposed in the SHINE design is presented in Table S1. The self-tracking concentrator is composed of 17.7 mm edge square Zeonex® E48R lenses concentrating the solar radiation on a 0.5 mm thick perforated steel slab filled with black wax (paraffin wax and carbon black or Sudan black). The infra-red radiation is absorbed by the black wax, which melts when irradiated by concentrated solar irradiation. The resulting volume change deforms a 2 µm dielectric layer located under a fused silica glass slab. The glass slab is used as a wave guide. The deformation of the dichroic layer ensures that the radiation at higher frequencies is reflected into the wave guide. Only a part of the infra-red spectrum is used for actuation, the unused part is assumed to be absorbed and cooled by the water circuit composed of copper pipes. The perforated steel plate containing the black wax is obtained using a 600 W laser and a piercing time of 0.25 s for each hole of 500 µm diameter. Paraffin wax is heated to 60°C and mixed with carbon black or Sudan black and then filled into the holes using a light vacuum at 60°C. A layer of PDMS is spin coated on top of it. The dielectric layer is sputtered on this layer and covered with another spin coated PDMS layer. A 1 mm thick float glass layer is placed under the steel plate to prevent the wax from leaving the device. Table S1 summarizes the CEDA of the different materials and processes needed to manufacture the concentrator. The data for the plasma etching process were estimated via the ecoinvent database.[1]

Table S1. CEDA and CGEA for the self-tracking SHINE concentrator.

Part	$CEDA_i$ (MJ m^{-2})	$CGEA_i$ ($kg_{CO2\text{-}eq}$ m^{-2})
Sputtering	488	49
Laser cutting	600	60
Plasma etching	20	6
PDMS	7	4
Steel	77	8
Silica fused glass	$1635/C$	$370 \cdot e$
Flat glass	38	3
Lenses	228	41
Wax	0	0
Copper pipes	179	143
Total	$1637 + 1635/C$	$314 + 185/C$

The data for sputtering was obtained using a report of Plasma Equipment Technical Services Incorporated (PETS Inc.) specifying sputtering rates, power, materials, and target area.* From this data, we estimated that a power density of 0.1 MW m^{-2} with a deposition rate of 4.2 Å s^{-1} was required to create the 2 µm thick dielectric layer. The average energy embodiment of common packaging polymers was considered for PDMS and Zeonex E48R®.[2] The energy embodiment of fused quartz was estimated as the sum of the energy embodiment of silica sand (which we obtained from the ecoinvent database) and the energy needed to melt it at the fabrication temperature of 2000°C.† As the thickness of the glass

*http://www.plasmaequip.com/Sputter%20Rates.pdf
†http://accuratus.com/fused.html

slab waveguide, e, depends on the desired concentration, the total CEDA of our concentrator was 1637 + 3270·e MJ m^{-2}. The reference area for the concentrator was 0.5 x 0.5 m^2, therefore the CEDA of the concentrator was 1637 + 1635/C MJ m^{-2}.
The CGEA for the self-tracking concentrator was obtained in two steps. The CGEAs of materials used to manufacture the device came from the ecoinvent database,[1] except for the PDMS (6.8 $kg_{CO2\text{-}eq}$ kg^{-1}) which was obtained from a report from Brandt et al.[3] The CGEAs of the processes used in the manufacturing of the SHINE concentrator – silica sand melting, sputtering, laser cutting, etching – were estimated assuming the energy needed for these processes was provided by electricity of the average EU energy mix with 0.1 $kg_{CO2\text{-}eq}$ MJ^{-1}.[4]

II. Model development

II.1 Electrical behavior of the photoabsorbers

The electrical behavior of GaInP/GaAs PV cells was given by the diode equation

$$i = i_{\mathrm{sc}} - i_{\mathrm{rec}}\left(e^{F_{\mathrm{F}}V/RT} - 1\right) \quad \text{(i)}$$

F_{F} is the Faraday constant and i the current density with respect to the PV area. The short circuit current i_{sc} = 146.2 A m^{-2} and the open circuit voltage V_{oc} = 2.69 V at AM 1.5 irradiance and 100% optical efficiency was calculated by the Shockley Queisser limit,[5,6] and were weighted to the yearly-averaged irradiance of Sevilla, Spain (Φ_1 = 223 W m^{-2}). The dark current, i_{rec}, was calculated as

$$i_{\mathrm{rec}} = i_{\mathrm{sc}} e^{-F_{\mathrm{F}}V_{\mathrm{oc}}/RT} \quad \text{(ii)}$$

The short circuit current behavior of a-Si/μc-Si/μc-Si PV cells was obtained by a phenomenological correlation combining two sets of reported experimental values.[7,8] The current-voltage relationship was given as

$$\frac{i}{i_{\mathrm{sc}}} = 1 + f - f\left(1 + \frac{1}{f}\right)^{\frac{V}{V_{\mathrm{oc}}}} \quad \text{(iii.a)}$$

$$f = 10^{-5}\ \frac{C\Phi}{\Phi_1}\left(\frac{C\Phi}{\Phi_1} + 1\right) \quad \text{(iii.b)}$$

This correlation was experimentally validated for C between 1 and 20 and was assumed valid for large C values.

II.2 Electrical behavior of the electrolyzer

The Electrolyzer load curve was given as

$$V = V_{\mathrm{o}} + \eta_{\mathrm{ohm}} + \eta_{\mathrm{act}} + \eta_{\mathrm{conc}} \quad \text{(iv)}$$

V_0 = 1.23 V and is the thermodynamic equilibrium potential required for the electrolysis of water at standard conditions, and j the current density with respect to the PEMEC area. Activation overpotential, η_{act}, is the sum of anodic and cathodic activation overpotentials. They were modeled using Tafel correlations

$$\eta_{\mathrm{act}} = \frac{RT}{2F_{\mathrm{F}}\alpha_{\mathrm{a}}} ln\left(1 + \frac{j}{j_{0,a}}\right) + \frac{RT}{2F_{\mathrm{F}}\alpha_{\mathrm{c}}} ln\left(1 + \frac{j}{j_{0,c}}\right) \quad \text{(v)}$$

$j_{0,a}$ and $j_{0,c}$ are the anodic and cathodic exchange current densities. Charge transfer coefficients $\alpha_a = 0.85$ and $\alpha_c = 1$ are selected for the anode and the cathode.[9]
Omhic losses, η_{ohm}, in the Nafion membrane with thickness $e_m = 50$µm and conductivity $\sigma = 10$ S m^{-1} were modeled using:

$$\eta_{\text{ohm}} = \frac{j e_{\text{m}}}{\sigma} \quad \text{(vi)}$$

Mass transport losses, η_{conc}, were modeled with the phenomenological equation from Kim et al.:[10]

$$\eta_{\text{conc}} = a e^{bj} \quad \text{(vii)}$$

The coefficients $a = 0.01$ V and $b = 5\ 10^{-4}$ m^2 A^{-1} were fitted to experimental results given by Dedigama et al.[11]
The resulting operating current and potential were obtained by an iterative process. Hydrogen mass production was calculated as:

$$\dot{m}_{\text{H2}} = \frac{j\, A_{\text{PEMEC}} M_{\text{H}_2}}{2 F_{\text{F}}}, \quad \text{(viii)}$$

with the electrode area A_{PEMEC}, and hydrogen molar mass $M_{H2} = 0.002$ kg mol^{-1}.

III. Additional figures

The variation of hydrogen production and power cost reduction of the device per unit area with changing concentration is depicted in Figure S1. Hydrogen production per unit area of the device decreased with concentration as a result of increasing overpotentials, and the power cost decreased with the decreasing contributions of the PV cells and the PEMEC to the device. EYR, the ratio of these two quantities, showed an optimum at C_{opt}. At this concentration, the design and operation of the device is the most sustainable.
Figure S2 shows that maximum EYR increased and C_{opt} decreased with increasing concentrator's optical efficiency. These results provide guidelines for the optimization of the SHINE concentrator.

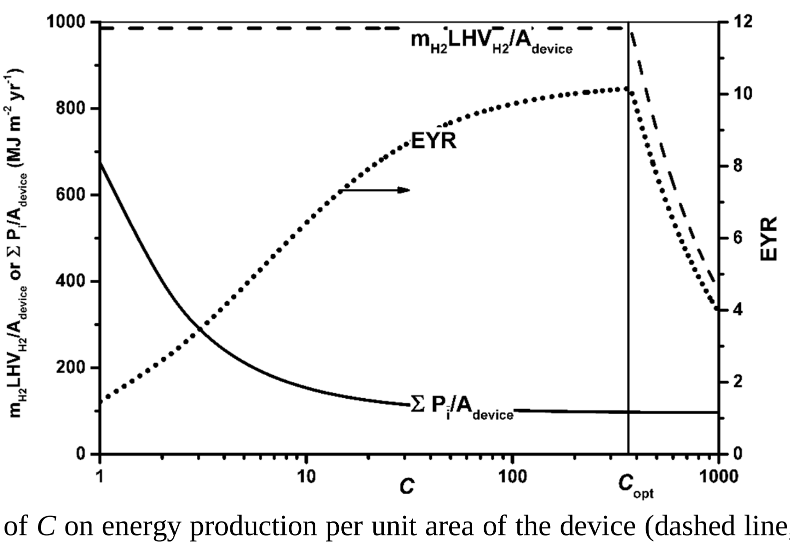

Figure S1. Effect of C on energy production per unit area of the device (dashed line, area-normalized nominator of eq. (1)), total power cost per unit area of the device (solid line), and EYR (dotted line) for the reference CPVE case. The optimal concentration $C_{opt} = 360$ is reached when the ratio between those quantities is maximized.

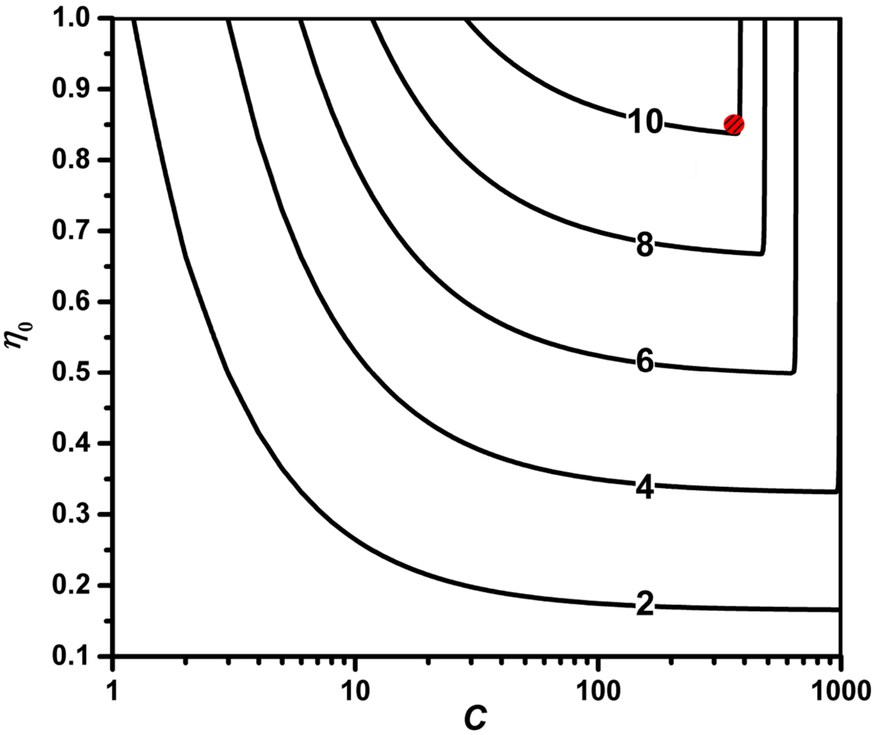

Figure S2. EYR contour lines as a function of concentration and optical efficiency for a CPVE using a GaInP/GaAs PV cell and the reference concentrator. The red dot indicates the reference concentrator with optical efficiency of 85%.

References

1. Ecoinvent V3.0, Swiss Center for Life Cycle Inventories, 2013.
2. M. D. Tabone, J. J. Cregg, E. J. Beckman, and A. E. Landis, *Environ. Sci. Technol.*, 2010, **44**, 8264–8269.
3. B. Brandt, E. Kletzer, H. Pilz, D. Hadzhiyska, and P. Seizov, Silicon-Chemistry Carbon Balance, *An assessment of greenhouse gas emissions and reductions*, Executive Summary comissioned by the Global Silicones Council, the Centre Européen des Silicones the Silicones Environmental, the Health and Safety Council of North America, and the Silicone Industry Association of Japan 2012.
4. B. Metz, L. Kuijpers, S. Solomon, O. O. Andersen, Stephen Davidson, J. Pons, D. de Jager, T. Kestin, M. Manningl, and L. Meyer, *Safeguarding the Ozone Layer and the Global Climate System: Issues Related to Hydrofluorocarbons and Perfluorocarbons*, Cambridge University Press, Cambridge, 2005.
5. W. Shockley and H. J. Queisser, *J. Appl. Phys.*, 1961, **32**, 510–519.
6. R. van de Krol and M. Grätzel, *Photoelectrochemical Hydrogen Production*, Springer US, Boston, MA, 2012, vol. 102.
7. L. M. van Dam, W. G. J. H. van Sark, Proceedings of the 2011 MRS Spring Meeting, San Francisco, 2011.
8. K. Söderström, G. Bugnon, R. Biron, C. Pahud, F. Meillaud, F.-J. Haug, and C. Ballif, *J. Appl. Phys.*, 2012, **112**, 114503–114507.
9. J. O. Bockris, A. Ammar, and S. Huq, *J. Phys. Chem*, 1957, **61**, 879–886.
10. J. Kim, S. Lee, S. Srinivasan, and C. E. Chamberlin, *J. Electrochem. Soc.*, 1995, **142**, 2670–2674.
11. I. Dedigama, K. Ayers, P. R. Shearing, and D. J. L. Brett, *Int. J. Electrochem. Sci.*, 2014, **9**, 2662–2681.